

1,2-Dibromo- and 1,2-Diiodotetrafluorobenzene as Precursors of Anionic Homo- and Heterometallic Gold Complexes

Eduardo J. Fernández,^{*,†} Antonio Laguna,[‡] Tania Lasanta,[†] José M. López-de-Luzuriaga,[†] Manuel Montiel,[†] and M. Elena Olmos[†]

Departamento de Química, Grupo de Síntesis Química de La Rioja, UA-CSIC, Complejo Científico Tecnológico, Universidad de la Rioja, 26001 Logroño, Spain, and Departamento de Química Inorgánica, Instituto de Ciencia de Materiales de Aragón, Universidad de Zaragoza-CSIC, 50009 Zaragoza, Spain

Received January 22, 2008

By reaction of LiR and [AuCl(tht)] the new organometallic compounds NBu₄[AuR₂] (R = 2-C₆BrF₄ (**1**), 2-C₆F₄I (**2**)) have been prepared. They react with TlPF₆ in different molar ratios yielding anionic extended chains with the stoichiometries {NBu₄[Tl₂(AuR₂)₃]}_n (R = 2-C₆BrF₄ (**3**), 2-C₆F₄I (**4**)) and {NBu₄[Tl(AuR₂)₂]}_n (R = 2-C₆BrF₄ (**5**), 2-C₆F₄I (**6**)). The crystal structures of **3** and **4** consist of anionic chains formed by association of loosely bound Au₂Tl₂ clusters interconnected by [AuR₂][−] anions via unsupported Au···Tl interactions, while **5** shows infinite polymetallic Au/Tl chains with an additional [AuR₂][−] fragment bonded to each Tl^I via unsupported Au···Tl contacts. The heterometallic bromotetrafluorophenyl complexes **3** and **5** display luminescence in the solid state, which is assigned to excited states that appear as result of the interactions between the metal centers. At 77 K different emissions appear in glassy solutions, which are assigned to the presence of oligomers of different length. In the case of the iodotetrafluorophenyl derivatives, in spite of presenting similar structures, complex **4** is weakly luminescent and complex **6** is nonluminescent both in the solid state at room temperature and at 77 K and in glassy solutions. This result is probably a consequence of the heavy-atom effect (HAE) due to the presence of iodine instead of bromine, which in the case of complex **4** provokes a reduction of the intensity if compared with its homologous compound **3** and which in **6** leads to the total quenching of the emission.

Introduction

The synthesis of supramolecular networks is nowadays one of the topics that is prompting more attention among the organometallic or coordination chemists due, among other factors, to the properties usually associated with those systems. Our group has contributed with a number of papers in which the structures and the optical properties associated with gold–heterometal interactions are studied. In fact, the supramolecular systems reported by us have a very rich structural diversity and intriguing photoluminescent properties, as well as, in some cases, potential applications as VOC sensors and luminescence signaling or, in others, as precursors of organic derivatives in potential catalytic reactions.^{1–19}

Among the reported methods that lead to these systems, one of the best known, which is employed in our laboratory, is the linkage of polyatomic anions or electron-rich molecules that undergo coordination to the binding sites of Lewis acids, leading to an enormous variety of extended structures.²⁰ Specifically, in our case, anionic gold precursors (bis(perhalophenyl)aurates) react with AgX (X = ClO₄, CF₃CO₂), CuCl, or TlX (X = NO₃, PF₆), which act as Lewis acids, giving rise to extended linear chains or two- or three-dimensional networks.^{1–3,5,6,8–14,16,17,19} In those studies, we have shown that the nature of the basic gold precursors is essential to the disposition that the metal centers display in the complexes and hence to the structure of

the networks and, consequently, to the optical properties associated with the structure in the solid state or even in solution. For instance, the reactions of NBu₄[AuR₂] (R = C₆F₅, C₆Cl₅) with TlPF₆ in the presence of neutral ligands lead to different dispositions of metals in the metallic chain or different coordination environments for the metal centers.^{1,3,5} In all cases the optical properties of these complexes are in agreement with those found in the theoretical calculations.

Another interesting characteristic that can be observed in these systems is the presence of secondary interactions that contribute to the stability of the polymeric systems in the majority of the complexes prepared following this strategy. These interactions usually appear between the heterometal and some of the halogen atoms of the perhalophenyl groups bonded to gold. In some cases these interactions occur with the nearest atoms of these rings, i.e. those placed in the ortho positions, but in others the interactions appear even with adjacent chains, which produces a three-dimensional network. For instance, that is the case of the complex [AuTl(C₆Cl₅)₂]_n, in which each thallium center has up to eight long Tl···Cl contacts.⁶ Presumably, these appear as a consequence of an electron deficiency at the thallium centers that is not saturated with neutral ligands.⁹

Therefore, it can be concluded from the previous comments that the steric and electronic properties associated with these perhalophenyl groups contribute to the metal–metal interactions, the structures, and, consequently, the optical properties of the heteronuclear materials.

Thus, following our current interest in knowing the different factors that condition the optical properties of the heteronuclear materials, we addressed the study to the preparation of new

* To whom correspondence should be addressed. E-mail: eduardo.fernandez@unirioja.es.

[†] Universidad de La Rioja.

[‡] Universidad de Zaragoza-CSIC.

homoleptic basic gold precursors and analyzed the influence of the aryl groups in the structures and optical properties in their reactions with thallium hexafluorophosphate. In addition, the number of organometallic homoleptic gold(I) complexes is very limited, and only five examples of the type $\text{NBu}_4[\text{AuR}_2]$ are known ($\text{R} = \text{C}_6\text{F}_5$, C_6Cl_5 , $\text{C}_6\text{Cl}_2\text{F}_3$, $\text{C}_6\text{F}_3\text{H}_2$, FMes).²¹

Thus, in this paper we report the synthesis of the two new gold precursors $\text{NBu}_4[\text{Au}(2\text{-C}_6\text{BrF}_4)_2]$ and $\text{NBu}_4[\text{Au}(2\text{-C}_6\text{F}_4\text{I})_2]$ and the study of their reactions with the acid salt TIPF_6 in different molar ratios, which lead in some cases to luminescent materials.

Results and Discussion

Synthesis and Characterization. The compounds $\text{NBu}_4[\text{Au}(2\text{-C}_6\text{BrF}_4)_2]$ (**1**) and $\text{NBu}_4[\text{Au}(2\text{-C}_6\text{F}_4\text{I})_2]$ (**2**) are obtained by reaction of $\text{Li}(2\text{-C}_6\text{FX})$ ($\text{X} = \text{Br}, \text{I}$) and $[\text{AuCl}(\text{tht})]$ following procedures similar to those reported for analogous complexes.²²

(1) Crespo, O.; Fernández, E. J.; Jones, P. G.; Laguna, A.; López-de-Luzuriaga, J. M.; Mendía, A.; Monge, M.; Olmos, E. *Chem. Commun.* **1998**, 2233.

(2) Fernández, E. J.; Gimeno, M. C.; Laguna, A.; López-de-Luzuriaga, J. M.; Monge, M.; Pyykkö, P.; Sundholm, D. *J. Am. Chem. Soc.* **2000**, *122*, 7287.

(3) Fernández, E. J.; Jones, P. G.; Laguna, A.; López-de-Luzuriaga, J. M.; Monge, M.; Pérez, J.; Olmos, M. E. *Inorg. Chem.* **2002**, *41*, 1056.

(4) Fernández, E. J.; López-de-Luzuriaga, J. M.; Monge, M.; Olmos, M. E.; Pérez, J.; Laguna, A. *J. Am. Chem. Soc.* **2002**, *124*, 5942.

(5) Fernández, E. J.; Laguna, A.; López-de-Luzuriaga, J. M.; Mendizábal, F.; Monge, M.; Olmos, M. E.; Pérez, J. *Chem. Eur. J.* **2003**, *9*, 456.

(6) Fernández, E. J.; López-de-Luzuriaga, J. M.; Monge, M.; Olmos, M. E.; Pérez, J.; Laguna, A.; Mohamed, A. A.; Fackler, Jr, J. P. *J. Am. Chem. Soc.* **2003**, *125*, 2022.

(7) Fernández, E. J.; Laguna, A.; López-de-Luzuriaga, J. M.; Olmos, E.; Pérez, J. *Chem. Commun.* **2003**, 1760.

(8) Fernández, E. J.; Laguna, A.; López-de-Luzuriaga, J. M.; Monge, M.; Montiel, M.; Olmos, M. E.; Pérez, J. *Organometallics* **2004**, *23*, 774.

(9) Fernández, E. J.; López-de-Luzuriaga, J. M.; Monge, M.; Montiel, M.; Olmos, M. E.; Pérez, J.; Laguna, A.; Mendizábal, F.; Mohamed, A. A.; Fackler, Jr, J. P. *Inorg. Chem.* **2004**, *43*, 3573.

(10) Fernández, E. J.; Laguna, A.; López-de-Luzuriaga, J. M.; Olmos, M. E.; Pérez, J. *Dalton Trans.* **2004**, 1801.

(11) Fernández, E. J.; Jones, P. G.; Laguna, A.; López-de-Luzuriaga, J. M.; Monge, M.; Montiel, M.; Olmos, M. E.; Pérez, J. *Z. Naturforsch.* **2004**, *59b*, 1379.

(12) Fernández, E. J.; Laguna, A.; López-de-Luzuriaga, J. M.; Monge, M.; Montiel, M.; Olmos, M. E. *Inorg. Chem.* **2005**, *44*, 1173.

(13) Fernández, E. J.; Laguna, A.; López-de-Luzuriaga, J. M.; Montiel, M.; Olmos, M. E.; Pérez, J. *Organometallics* **2005**, *24*, 1631.

(14) Fernández, E. J.; Laguna, A.; López-de-Luzuriaga, J. M.; Montiel, M.; Olmos, M. E.; Pérez, J. *Inorg. Chim. Acta* **2005**, *358*, 4293.

(15) Fernández, E. J.; López-de-Luzuriaga, J. M.; Olmos, M. E.; Pérez, J.; Laguna, A.; Lagunas, M. C. *Inorg. Chem.* **2005**, *44*, 6012.

(16) Fernández, E. J.; Laguna, A.; López-de-Luzuriaga, J. M.; Montiel, M.; Olmos, M. E.; Pérez, J. *Organometallics* **2006**, *25*, 1689.

(17) Fernández, E. J.; Laguna, A.; López-de-Luzuriaga, J. M.; Monge, M.; Montiel, M.; Olmos, M. E.; Rodríguez-Castillo, M. *Organometallics* **2006**, *25*, 3639.

(18) Fernández, E. J.; Laguna, A.; López-de-Luzuriaga, J. M.; Monge, M.; Montiel, M.; Olmos, M. E. *Inorg. Chem.* **2007**, *46*, 2953.

(19) Fernández, E. J.; Jones, P. G.; Laguna, A.; López-de-Luzuriaga, J. M.; Monge, M.; Olmos, M. E.; Puelles, R. C. *Organometallics* **2007**, *26*, 5931.

(20) (a) Hawthorne, M. F.; Zheng, Z. *Acc. Chem. Res.* **1997**, *30*, 267. (b) Hawthorne, M. F. *Pure Appl. Chem.* **1994**, *66*, 245. (c) Wuest, J. D. *Acc. Chem. Res.* **1999**, *32*, 81. (d) Vaugeois, J.; Simard, M.; Wuest, J. D. *Coord. Chem. Rev.* **1995**, *95*, 55.

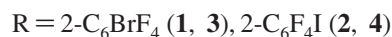
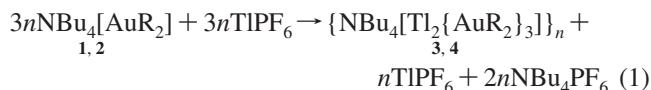
(21) (a) Laguna, A.; Gimeno, M. C. *Trends Organomet. Chem.* **1994**, *1*, 231. (b) Schmidbaur, H.; Grohmann, A.; Olmos, M. E.; Schier, A. In *The Chemistry of Organic Derivatives of Gold and Silver*; Patai, S.; Rappaport, Z., Eds.; Wiley: Chichester, U.K., 1999; pp 227–331. (c) Schmidbaur, H.; Grohmann, A.; Olmos, M. E. In *The Chemistry of Organic Derivatives of Gold and Silver*; Schmidbaur, H., Ed.; Wiley: Chichester, U.K., 1999; pp 648–746. (d) Fernández, E. J.; Laguna, A.; Olmos, M. E. *Adv. Organomet. Chem.* **2005**, *52*, 77.

(22) Usón, R.; Laguna, A.; Vicente, J. *Synth. React. Inorg. Met.-Org. Chem.* **1977**, *7*, 463.

Analytical and spectroscopic data of both complexes agree with the proposed stoichiometries (see the Experimental Section). Their IR spectra show, among others, absorptions at 1612, 1594, 1078, and 817 cm^{-1} in **1** and 1609, 1587, 1076, and 806 cm^{-1} in **2**, arising from the presence of a pentahalophenyl group bonded to gold(I), and at 880 cm^{-1} from NBu_4^+ in both of them. The presence of NBu_4^+ is also confirmed in their ^1H NMR spectra in CDCl_3 , which display signals corresponding to the proton resonances of the cation in this solvent, and even in their mass (ES^+) spectra, in which the parent peak appears at m/z 242. Mass spectra (ES^-) show signals corresponding to $[\text{Au}(2\text{-C}_6\text{FX})_2]^-$ ($\text{X} = \text{Br}$ (**1**) at m/z 653 and $\text{X} = \text{I}$ (**2**) at m/z 747) with the expected isotopic distributions. In addition, the ^{19}F NMR spectra of both complexes, **1** and **2**, show patterns corresponding to four types of inequivalent fluorine atoms, which appear as doublets of doublets due to the small value of the coupling constants between fluorine atoms in positions meta to gold.²³ However, when a halogen in an ortho position relative to gold is replaced by a different halogen, it produces a deshielding of the fluorine atoms in a position meta to gold. When the ^{19}F NMR spectra of complexes **1** and **2** are compared, this effect can be seen in the position corresponding to the fluorine atom located in an ortho position with respect to the bromo or iodo center, and thus, it suffers a shift to lower field as the electronegativity of the new halogen in an ortho position decreases.

Both of these compounds are soluble in acetone, tetrahydrofuran, halogen solvents, and alcohols and insoluble in *n*-hexane, diethyl ether, and water. In addition, these complexes slowly decompose in solution, generating gold mirrors after having been exposed to light for hours.

Treatment of $\text{NBu}_4[\text{Au}(2\text{-C}_6\text{BrF}_4)_2]$ (**1**) with equimolecular amounts of TIPF_6 in tetrahydrofuran and subsequent concentration under vacuum produces a yellow greenish solid. Addition of dichloromethane allows the separation of a white solid, which is separated by filtration and identified as TIPF_6 . The solution is concentrated under vacuum and then toluene is added, leading to the precipitation of NBu_4PF_6 , which is filtered off. Evaporation of the solvent to dryness affords complex **3**, which is isolated as a pale green solid with the stoichiometry $\{\text{NBu}_4[\text{Ti}_2\{\text{Au}(2\text{-C}_6\text{BrF}_4)_2\}_3]\}_n$ (see eq 1).



Complex **3** is stable to air and moisture, luminescent under ultraviolet radiation, soluble in tetrahydrofuran, acetone, toluene, and dichloromethane, and insoluble in diethyl ether, alcohols, or *n*-hexane. Its IR spectrum shows, among others, absorptions at 1617, 1595, 1088, and 823 cm^{-1} arising from the presence of 2-bromotetrafluorophenyl groups bonded to gold(I) and at 883 cm^{-1} due to the presence of NBu_4^+ , also confirmed in its ^1H NMR spectrum in CDCl_3 , which displays signals at 3.22 (m, 2H, CH_2), 1.65 (m, 2H, CH_2), 1.39 (m, 2H, CH_2), and 0.98 ppm (t, 3H, CH_3). Its ^{19}F NMR spectrum in CDCl_3 shows the resonances corresponding to four types of inequivalent fluorine atoms at -113.4 , -127.8 , -158.5 , and -160.6 ppm, chemical shifts similar to those of the starting material (**1**). Compound **3** dissociates in solution, and it shows a conductivity near to that

(23) Albéniz, A. C.; Casado, A. L.; Espinet, P. *Organometallics* **1997**, *16*, 5416.

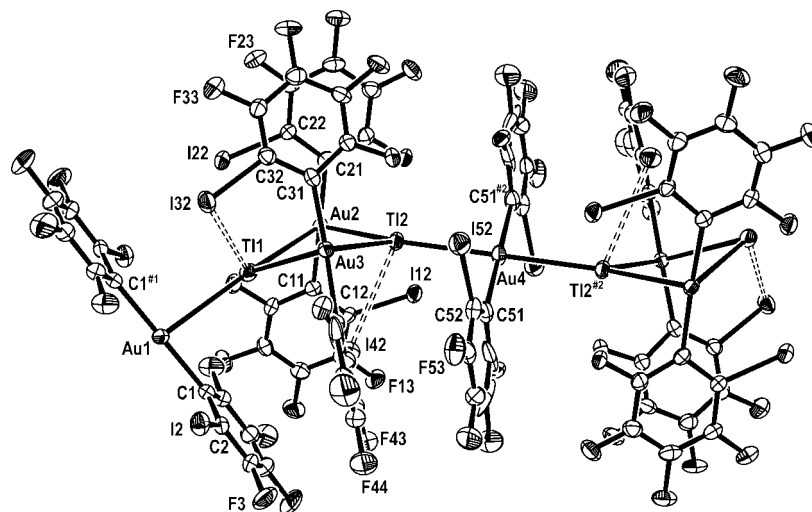


Figure 2. Structure of the anion of complex **4** (30% probability level) with the labeling scheme of the atom positions. H atoms are omitted for clarity.

Table 1. Selected Bond Lengths (Å) and Angles (deg) for Complex **3**^a

Au(1)–C(1)	2.050(9)	Au(1)–Tl(2)#1	3.0127(5)
Au(1)–C(11)	2.053(9)	Au(1)–Tl(1)	3.0355(5)
Au(2)–C(21)	2.061(9)	Au(2)–Tl(2)	3.0832(5)
Au(2)–C(31)	2.070(9)	Au(2)–Tl(1)	3.1247(5)
Au(3)–C(51)	2.027(10)	Au(3)–Tl(2)	3.0924(5)
Au(3)–C(41)	2.038(10)	Au(3)–Tl(1)	3.1021(5)
C(1)–Au(1)–C(11)	178.3(3)	Au(1)–Tl(1)–Au(3)	122.993(15)
Tl(2)#1–Au(1)–Tl(1)	169.408(17)	Au(1)–Tl(1)–Au(2)	138.145(16)
C(21)–Au(2)–C(31)	175.0(3)	Au(3)–Tl(1)–Au(2)	90.719(13)
Tl(2)–Au(2)–Tl(1)	85.622(13)	Au(1)#2–Tl(2)–Au(2)	151.924(16)
C(51)–Au(3)–C(41)	175.1(4)	Au(1)#2–Tl(2)–Au(3)	112.319(15)
Tl(2)–Au(3)–Tl(1)	85.854(13)	Au(2)–Tl(2)–Au(3)	91.685(13)

^a Symmetry transformations used to generate equivalent atoms: (#1) $x + 1/2, y, -z + 1/2$; (#2) $x - 1/2, y, -z + 1/2$.

Table 2. Selected Bond Lengths (Å) and Angles (deg) for Complex **4**^a

Au(1)–C(1)	2.061(12)	Au(1)–Tl(1)	3.3644(6)
Au(2)–C(11)	2.034(11)	Tl(1)–Au(3)	3.0682(7)
Au(2)–C(21)	2.044(12)	Tl(1)–Au(2)	3.4659(8)
Au(3)–C(31)	2.048(13)	Au(2)–Tl(2)	3.1213(6)
Au(3)–C(41)	2.097(11)	Tl(2)–Au(4)	2.9956(5)
Au(4)–C(51)	2.066(12)	Tl(2)–Au(3)	3.0791(7)
C(1)–Au(1)–C(1)#1	180.0(5)	Tl(2)–Au(4)–Tl(2)#2	180.0
Tl(1)#1–Au(1)–Tl(1)	180.00(3)	Au(3)–Tl(1)–Au(1)	108.41(2)
C(11)–Au(2)–C(21)	173.4(4)	Au(3)–Tl(1)–Au(2)	87.567(18)
Tl(2)–Au(2)–Tl(1)	82.320(16)	Au(1)–Tl(1)–Au(2)	162.75(2)
C(31)–Au(3)–C(41)	168.8(4)	Au(4)–Tl(2)–Au(3)	120.568(19)
Tl(1)–Au(3)–Tl(2)	89.91(2)	Au(4)–Tl(2)–Au(2)	145.38(2)
C(51)#2–Au(4)–C(51)	180.000(2)	Au(3)–Tl(2)–Au(2)	93.877(17)

^a Symmetry transformations used to generate equivalent atoms: (#1) $-x, -y, -z$; (#2) $-x + 1, -y, -z + 1$.

ligand).^{2,17,24} However, in the latter the Au₂M₂ units are more planar than in the thallium complexes and associate through Au...Au interactions instead of via Au...M contacts. In complex **3** the Au–Tl distances within the tetranuclear units are of the same order, lying in the range 3.0832(5)–3.1247(5) Å, and are close to those found in similar Au₂Tl₂ units^{4,13,15} but slightly longer than the Au–Tl interactions that join the Au₂Tl₂ fragments and the bridging bis(perhalophenyl)aurate(I) anions (3.0127(5) and 3.0355(5) Å). The latter compare well with those observed in most of the polymeric species with unsupported Au...Tl interactions.^{1,3,5,6,8–11,13} In contrast, the

Au–Tl lengths in **4** are more dissimilar, both within the Au₂Tl₂ cores (3.0682(7)–3.4659(8) Å) and between the tetranuclear units and the [Au(C₆F₄I)₂][–] fragments (2.9956(5) and 3.3644(6) Å), the longest one being of the same order as the Au–Tl distances found in the pentachlorophenyl derivatives [{Tl₂(THF)₂(μ-4,4'-bipy)}{Au(C₆Cl₅)₂}]_n (3.4800(3) Å) or [{Tl(2,2'-bipy)}{Au(C₆Cl₅)₂}]_n (3.4899(6) Å).¹¹ The presence of aurophilic interactions within the clusters can be ruled out, since the shortest metal–metal distance between gold(I) centers (Au(2)–Au(3) = 4.431 (**3**), 4.530 Å (**4**)) is longer than twice its van der Waals radius (3.32 Å).

The bond lengths and angles within the tetranuclear units are, in general, similar to those found in the Au₂Tl₂ loosely bound clusters previously reported,^{4,13,15} with Au–C distances ranging between 2.027(10) and 2.070(9) Å in **3** and between 2.034(11)

(24) (a) Usón, R.; Laguna, A.; Laguna, M.; Jones, P. G.; Sheldrick, G. M. *Chem. Commun.* **1981**, 1097. (b) Usón, R.; Laguna, A.; Laguna, M.; Manzano, B. R.; Jones, P. G.; Sheldrick, G. M. *J. Chem. Soc., Dalton Trans.* **1984**, 285.

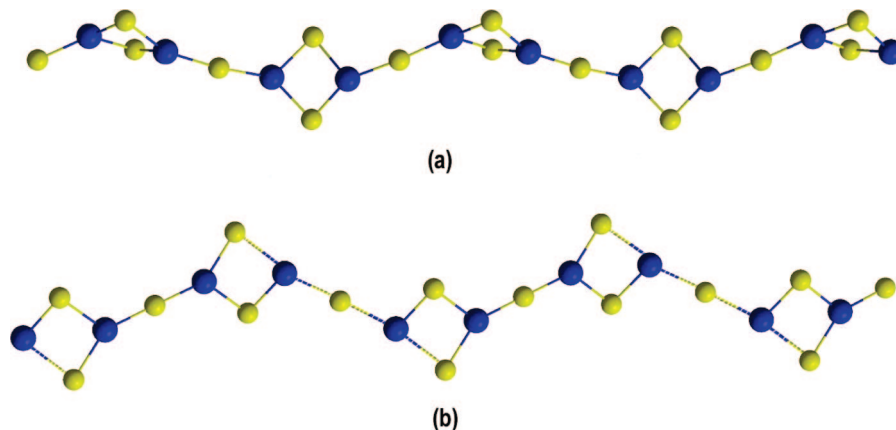


Figure 3. Polymetallic chain of complexes (a) **3** and (b) **4** with the $[\text{Au}(\text{C}_6\text{F}_4\text{X})_2]^-$ anions acting as bridging metallo ligands: (yellow) gold; (blue) thallium.

and 2.097(11) Å in **4** and the Au–C bond lengths corresponding to the bridging $[\text{Au}(\text{C}_6\text{F}_4\text{X})_2]^-$ fragments lying within these ranges (see Tables 1 and 2). As in the anionic polymer $\{\text{NBu}_4[\text{Tl}_2\{\text{Au}(\text{C}_6\text{Cl}_5)_2\}\{\mu\text{-Au}(\text{C}_6\text{Cl}_5)_2\}_2]\}_n$,¹³ the gold(I) centers of the tetranuclear units in **4** display a more distorted linear environment ($\text{C–Au–C} = 168.8(4), 173.4(4)^\circ$) than in the previous examples ($\text{C–Au–C} = 173.7(2)–178.0(2)^\circ$)^{4,15} or than in **3** ($\text{C–Au–C} = 175.0(3), 175.1(4)^\circ$), while the $[\text{Au}(\text{C}_6\text{BrF}_4)_2]^-$ fragments that join two Au_2Tl_2 units contain perfectly linear two-coordinate gold atoms (if the intermetallic interactions are not considered). The M–M'–M angles within the Au_2Tl_2 units (see Tables 1 and 2) compare well with those found in complex $\{\text{NBu}_4[\text{Tl}_2\{\text{Au}(\text{C}_6\text{Cl}_5)_2\}\{\mu\text{-Au}(\text{C}_6\text{Cl}_5)_2\}_2]\}_n$ ¹³ and differ slightly from those observed in the loosely bound butterfly Au_2Tl_2 clusters previously described,^{4,15} showing wider Tl–Au–Tl and narrower Au–Tl–Au angles, which avoids the formation of $\text{Tl}\cdots\text{Tl}$ interactions (Tl–Tl : 4.219 (**3**) and 4.530 Å (**4**)) that are present in discrete Au_2Tl_2 clusters (Tl–Tl : 3.6027(6)–3.7152(4) Å).^{4,15}

The coordination sphere of the Tl atoms in these two complexes is almost planar (sum of Au–Tl–Au angles of Tl(I) of 351.9 and 355.9° (**3**) or 359.8 and 358.7° (**4**)) with a nearly T-shape environment for Tl1 in **4** (see Table 2). Thus, the stereoactivity of the inert pair, usually stereochemically active,²⁵ is not apparent in these cases. The main difference between these two structures is the disposition of the tetranuclear units in the polymeric chain, which form an angle of about 70° in **3** while they are nearly parallel in **4**, as shown in Figure 3.

Finally, it is worth noting that the thallium centers maintain interactions with some of the heavier halogens. Thus, in **3** there are two $\text{Tl}\cdots\text{Br}$ contacts of 3.3924(13) and 3.4587(11) Å for $\text{Tl2}\cdots\text{Br42}$ and $\text{Tl1}\cdots\text{Br22}$, respectively, shorter than in $[\text{Tl}(1,4\text{-dioxane})][\text{TlBr}_4]$ (3.564 Å)²⁶ or in $\text{Tl}_2[\text{fac-Os}(\text{CO})\text{Br}_2\text{F}_3]$ (3.294–3.540 Å)²⁷ and identical to the shortest contact in $[\text{Tl}(\eta^6\text{-toluene})_2](\text{Br}_6\text{CB}_{11}\text{H}_6)$ (3.393 and 3.592 Å),²⁸ where the bromine atoms act as bridges between two thallium centers, thus forming a dimer. There are also two $\text{Tl}\cdots\text{I}$ interactions of 3.4749(11) and 3.4701(15) Å in complex **4** for $\text{Tl1}\cdots\text{I32}$ and $\text{Tl2}\cdots\text{I42}$, respectively, which are shorter than in $\{\text{C}_5\text{Me}_5\text{RhI}[\mu_2\text{-}$

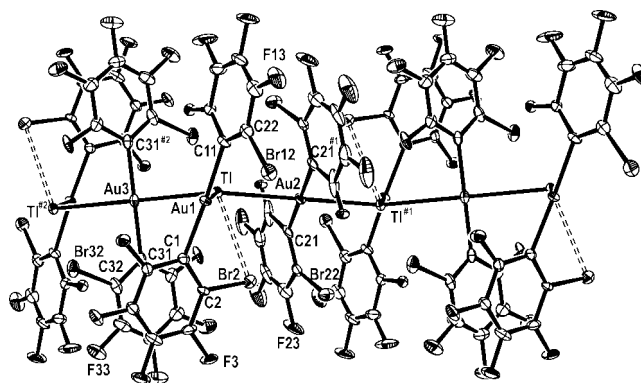


Figure 4. Structure of the anion of complex **5** (30% probability level) with the labeling scheme of the atom positions. H atoms are omitted for clarity.

$\text{P}(\text{O})(\text{OMe})_2\}_2\text{Tl}^{29}$ (3.537 Å) and, considering the van der Waals radii of bromine (1.85 Å) and iodine (1.98 Å),³⁰ are stronger than the $\text{Tl}\cdots\text{Br}$ contacts in **3**, which seem to have an important effect on the optical properties of these products (see below).

The crystal structure of complex **5** was also determined from single crystals obtained by slow diffusion of *n*-hexane into a saturated solution of the complex in a mixture of toluene and THF (2:1). It can be seen as an infinite polymetallic Au/Tl chain formed via unsupported $\text{Au}\cdots\text{Tl}$ interactions in which each thallium(I) center binds a terminal $[\text{Au}(\text{C}_6\text{BrF}_4)_2]^-$ fragment also via a $\text{Au}\cdots\text{Tl}$ contact (see Figures 4 and 5), thus forming anionic chains which run parallel to the crystallographic *x* axis. The separations between the metals that form the polymetallic chain, of 3.0054(4) and 3.0216(4) Å, are slightly longer than the intermetallic distance between thallium and the terminal $[\text{Au}(\text{C}_6\text{BrF}_4)_2]^-$ group (2.9354(6) Å), and all of them lie within the range of Au–Tl distances observed in most of the polymeric species with unsupported $\text{Au}\cdots\text{Tl}$ interactions (Table 3).^{1,3,5,6,8–11}

As in the case of complex **4**, as well as in the related complexes $\{\text{NBu}_4[\text{Tl}_2\{\text{Au}(\text{C}_6\text{Cl}_5)_2\}\{\mu\text{-Au}(\text{C}_6\text{Cl}_5)_2\}_2]\}_n$, $\{\text{NBu}_4[\text{Tl}\{\text{Au}(3,5\text{-C}_6\text{Cl}_2\text{F}_3)_2\}_2]\}_n$, and $\{\text{NBu}_4[\text{Tl}\{\text{Au}(\text{C}_6\text{Cl}_5)_2\}\{\text{Au}(3,5\text{-C}_6\text{Cl}_2\text{F}_3)_2\}_2]\}_n$,¹³ the Au(I) atoms of the main chain display a perfectly linear (if the intermetallic interactions are not taken into account) or square-planar environment (if they are consid-

(25) Kristiansson, O. *Eur. J. Inorg. Chem.* **2002**, 2355.

(26) Marsh, R. E.; Herbstein, F. H. *Acta Crystallogr., Sect. B: Struct. Crystallogr., Cryst. Chem.* **1988**, *44*, 77.

(27) Bernhardt, E.; Preetz, W. Z. *Anorg. Allg. Chem.* **1998**, 624–694.

(28) Mathur, R. S.; Drovetskaya, T.; Reed, C. A. *Acta Crystallogr., Sect. C: Cryst. Struct. Commun.* **1997**, *53*, 881.

(29) Valderrama, M.; Scotti, M.; Campos, P.; Werner, H.; Müller, G. *Chem. Ber.* **1990**, *123*, 1005.

(30) Source: <http://www.webelements.com/>.

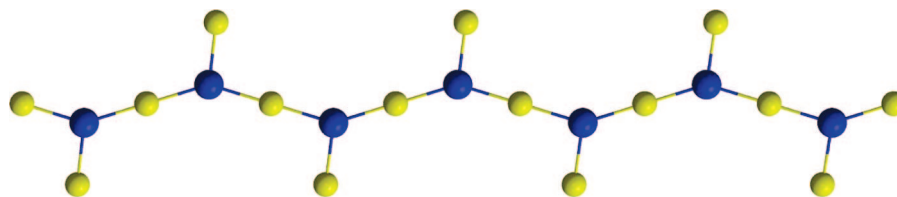


Figure 5. Polymetallic chain of complex **5** with the $[\text{Au}(\text{C}_6\text{BrF}_4)_2]^-$ anions acting as terminal metallo ligands: (yellow) gold; (blue) thallium.

Table 3. Selected Bond Lengths (Å) and Angles (deg) for Complex **5**^a

Au(1)–C(1)	2.072(13)	Au(1)–Tl	2.9354(6)
Au(1)–C(11)	2.079(12)	Tl–Au(2)	3.0054(4)
Au(2)–C(21)	2.091(15)	Tl–Au(3)	3.0216(4)
Au(3)–C(31)	2.067(15)		
C(1)–Au(1)–C(11)	173.8(4)	Au(1)–Tl–Au(2)	113.323(17)
C(21)–Au(2)–C(21)#1	180.000(2)	Au(1)–Tl–Au(3)	98.505(16)
Tl#1–Au(2)–Tl	180.000(19)	Au(2)–Tl–Au(3)	145.637(17)
C(31)–Au(3)–C(31)#2	180.000(2)	Tl–Au(3)–Tl#2	180.0

^a Symmetry transformations used to generate equivalent atoms: (#1) $-x, -y + 1, -z + 1$; (#2) $-x + 1, -y + 1, -z + 1$.

ered), while those present in the terminal $[\text{Au}(\text{C}_6\text{BrF}_4)_2]^-$ units show a C–Au–C angle of 173.8(4)°.

If the intermetallic contacts are considered, the coordination sphere of the Tl atoms in this complex is, as in **3** and **4**, almost planar (sum of Au–Tl–Au angles of 357.5°) with a distorted-trigonal-planar environment. Again, the inert electron pair in Tl(I) seems to be stereochemically nonactive in this case, which is not the usual case.

Finally, there are intramolecular Tl⋯Br interactions of 3.3722(19) Å, even shorter than in complex **3**, as well as intermolecular contacts of 3.4455(21) Å between the thallium centers of a chain and a bromine atom of an adjacent polymer, which probably contribute to the stability of the system.

Optical Properties. In addition to the interesting structures, some of the complexes display a brilliant luminescence when they are irradiated with UV light in solid state, but others are weakly luminescent or even are not luminescent, in spite of having similar structures. Thus, the bromoaryl complexes $\{\text{NBu}_4[\text{Tl}_2(\text{Au}(2\text{-C}_6\text{BrF}_4)_2)_3]\}_n$ (**3**) and $\{\text{NBu}_4[\text{Tl}(\text{Au}(2\text{-C}_6\text{BrF}_4)_2)_2]\}_n$ (**5**) display a strong luminescence at room temperature at 500 nm (excitation at 400 nm) for **3** and 520 nm (excitation at 420 nm) for **5**, respectively, independent of the excitation wavelengths. At 77 K in the solid state the emissions red-shift, appearing at 515 nm (excitation at 400 nm) and 560 nm (excitation at 475 nm), respectively (see Figure 6). In addition, the lifetimes of both complexes in the solid state at room temperature display a monoexponential decay with values of 10.5 μs ($R^2 = 0.993$) (**3**) and 10.9 μs ($R^2 = 0.991$) (**5**), in accordance with phosphorescent processes.

Both complexes lose these emissions when they are dissolved, recovering them when the solvent is evaporated. Instead, in dilute tetrahydrofuran solutions weak emissions at 425 nm, which are also observed in the precursor gold complex $\text{NBu}_4[\text{Au}(2\text{-C}_6\text{BrF}_4)_2]$ (**1**), appear. Therefore, these new emissions are likely to be due to $\pi\pi^*$ transitions located in the perhalophenyl rings. In accordance with this, the UV–vis spectra of these heterometallic complexes and the gold precursor in deoxygenated tetrahydrofuran show similar features with absorptions of high

energy below 350 nm and a maximum at 291 nm. In addition, other heterometallic gold–thallium complexes with the related aryl group C_6F_5 also show UV–vis spectra with similar features and with high-energy bands between 250 and 325 nm and a maximum absorption at 275 nm, which were said to have a similar origin.¹⁴ In addition, as we have noted above in Synthesis and Characterization, neither the spectroscopic data (NMR, MS) nor the molar conductivity measurements indicate association between the different ionic counterparts in solution.

The absence of low-energy emissions in solution for these types of heteronuclear extended systems is not rare.³¹ In fact, the only exceptions to this behavior appear in systems that show Tl^I–Tl^I interactions in the solid state.^{4,8,14,15} In our case, complex **3** is the one that shows the thallium centers at a shorter distance (4.291 Å), although they are far from the sum of their van der Waals radii. Thus, from these comments, it seems likely that the gold–thallium interactions are the main contributors to the emissive excited states.

Nevertheless, taking the structural data into account, we cannot establish a relationship between the metal–metal distances and the emission energies for both complexes. For instance, the shortest Au–Tl distance in complex **5** (2.9354(7) Å) does not lead to the lowest energy emission. In addition, previous TD-DFT calculations carried out for related heteronuclear gold–thallium complexes point out the anionic $[\text{AuR}_2]^-$ fragments as the origin of the electronic transitions with a high contribution of the perhalophenyl groups.^{3,5,6} Therefore, the emitting states responsible for the luminescence in the solid state for these complexes are likely to arise from a mixture of metal (gold) to metal (thallium) charge transfer (MMCT) and ligand (perhalophenyl) to metal (gold–thallium) charge transfer (LMCT).

In the case of frozen dilute solutions at 77 K, both products display similar emissions. Glassy EtOH/MeOH (4:1; 5×10^{-4} M) solutions of both complexes show emissions at 425 and 490 nm by excitation at 310–360 nm, the first one appearing as a shoulder of the less energetic emission (see Figure 7).

This 425 nm band also appears in the precursor $\text{NBu}_4[\text{Au}(2\text{-C}_6\text{BrF}_4)_2]$ (**1**) under the same conditions. Consequently, similarly to what happened in solution at room temperature, it is likely to be due to $\pi\pi^*$ transitions located in the perhalophenyl rings. In contrast, the low-energy emission can be assigned to a smaller oligomer that appears in both complexes as a consequence of the rapid cooling of the solutions. Similar results are obtained when the solutions are prepared with THF as solvent at 77 K; therefore, the formation of exciplexes with the solvent in the excited state can be ruled out. Another plausible explanation could arise from the Br⋯Tl interaction that appears in both crystal structures, which could lead to an LMCT transition for the low-energy emissions. Nevertheless, the different lengths of the Au⋯Tl interactions observed in both complexes do not seem to influence the excited states responsible for the emissions.

In the case of the complexes $\{\text{NBu}_4[\text{Tl}_2(\text{Au}(2\text{-C}_6\text{F}_4)_2)_3]\}_n$ (**4**) and $\{\text{NBu}_4[\text{Tl}(\text{Au}(2\text{-C}_6\text{F}_4)_2)_2]\}_n$ (**6**) and in spite of the similarity of the stoichiometries to those of the aforementioned

(31) (a) Fernández, E. J.; Laguna, A.; López-de-Luzuriaga, J. M. *Gold Bull.* **2001**, *34* (1), 14. (b) Fernández, E. J.; Laguna, A.; López-de-Luzuriaga, J. M. *Coord. Chem. Rev.* **2005**, *249*, 1423. (c) Fernández, E. J.; Laguna, A.; López-de-Luzuriaga, J. M. *Dalton Trans.* **2007**, 1969.

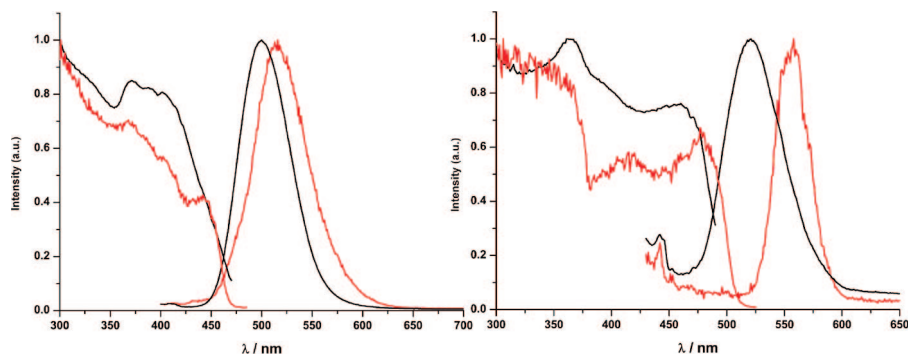


Figure 6. Corrected excitation and emission spectra of complexes **3** (left) and **5** (right) at room temperature (black line) and at 77 K (red line).

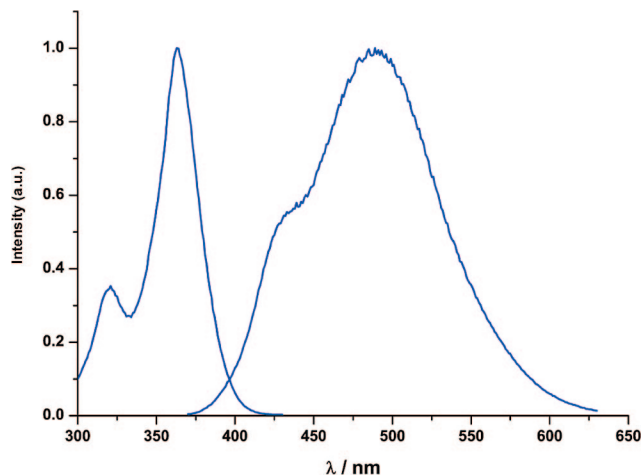


Figure 7. Corrected excitation and emission spectra of complex **3** in glassy EtOH/MeOH (4:1) solution at 77 K.

complexes **3** and **5**, each shows a very different optical behavior. Thus, complex **4** is weakly luminescent in the solid state and complex **6** does not display any emission. For example, complex **4** shows an emission at 555 nm (excitation at 450 nm) in the solid state, which is independent of the excitation wavelength and the temperature (emission at 555 nm at 77 K).

The interesting rigidochromism in the solid state is assigned by some authors to a rigidity in the structure that prevents the decrease of the metal–metal distances when the temperature is lowered.³² In this case, it is worth noting that the structure displays short Tl^I–I contacts that probably contribute to shorten the Au–Tl distances, which is difficult when the temperature is lowered.

As before, the emission at 555 nm disappears when the measurements are carried out in solution at room temperature and it is regenerated when the solvent is evaporated, which is indicative of the influence of the metal–metal interactions in the excited state. Both complexes display similar UV–vis spectra, which is interpreted as a dissociation into the cationic and anionic counterparts provoked by the solvent. In frozen THF or EtOH/MeOH (4:1) at 77 K it displays an emission at 495 nm (excitation at 365 nm) that is likely to be attributed to oligomers formed as a consequence of the cooling of the solutions.

In contrast, interestingly, this complex in solution does not show emissions in the blue region, as in the case of complexes

3 and **5**. Neither does the precursor $\text{NBu}_4[\text{Au}(2\text{-C}_6\text{F}_4\text{I})_2]$ (**2**), which does not display any luminescence in solution at room temperature or at 77 K. This fact or even the absence of luminescence for complex **6** is likely to be due to an iodide heavy-atom effect (HAE), which in the case of complex **4** provokes a reduction of the intensity if compared with the homologous complex **3** and that in complex **6** leads to the total quenching of the emission. In fact, recently, Omary et al. reported a study about the influence of the heavy-atom effect on the luminescence of the adducts of the 1-halonaphthalene series with perfluoro-*o*-phenylenemercury.³³ In this paper it was suggested that the synergy of the internal iodide HAE with the external mercury HAE led to quenching vs unsubstituted naphthalene, due to a larger nonradiative decay rate constant (k_{nr}) at room temperature. This was in contrast to the situation in the bromo and chloro analogues, where this synergy led to an enhancement vs unsubstituted naphthalene due to a larger radiative decay rate constant (k_r) at room temperature.

Experimental Section

Instrumentation. Infrared spectra were recorded in the 4000–200 cm^{-1} range on a Nicolet Nexus FT-IR instrument using Nujol mulls between polyethylene sheets. C, H, N analyses were carried out with a Perkin-Elmer 240C microanalyzer. Mass spectra were recorded on a HP5989B API-Electrospray spectrometer. ¹H and ¹⁹F NMR spectra were recorded on a Bruker ARX 300 spectrometer in CDCl_3 or THF-*d*₈ solutions. Chemical shifts are quoted relative to SiMe_4 (¹H, external) and CFCl_3 (¹⁹F, external). Excitation and emission spectra were recorded with a Jobin-Yvon Horiba Fluorolog 3-22 Tau-3 spectrofluorimeter. Phosphorescence lifetimes were recorded with a Fluoromax phosphorimeter accessory containing a UV xenon flash tube with a flash rate between 0.05 and 25 Hz. The lifetime data were fitted using the Jobin-Yvon software package and the Origin 6.1 program.

General Comments. Thallium(I) hexafluorophosphate, *o*- $\text{C}_6\text{Br}_2\text{F}_4$, and *o*- $\text{C}_6\text{BrF}_4\text{I}$ are commercially available and were purchased from Aldrich. Solvents were freshly distilled under argon prior to use, and all the reactions were carried out under argon.

Synthesis of $\text{NBu}_4[\text{Au}(2\text{-C}_6\text{BrF}_4)_2]$ (1**).** To a diethyl ether solution of $\text{Li}(2\text{-C}_6\text{BrF}_4)$ (30 mmol) at 203 K was added $[\text{AuCl}(\text{tht})]^{34}$ (3.20 g, 10 mmol). After 1 h of stirring, NBu_4Br (4 g, 12.5 mmol) was added and the reaction mixture was stirred at 203 K for 40 min. After 8–10 h of stirring at room temperature, a white solid was separated by filtration and washed with water (3×5 mL), diethyl ether (3×5 mL), and *n*-hexane (3×5 mL). The solid was solved in dichloromethane and the solution concentrated

(32) (a) Wrighton, M.; Morse, D. L. *J. Am. Chem. Soc.* **1974**, *96*, 998. (b) Wang, S.; Garzón, G.; King, C.; Wang, J. C.; Fackler, J. P., Jr. *Inorg. Chem.* **1989**, *28*, 4623. (c) Itokazu, M. K.; Polo, A. S.; Iha, N. Y. M. *J. Photochem. Photobiol. A: Chem.* **2003**, *160*, 27.

(33) Elbjerrami, O.; Burrell, C. M.; Gabbai, F. P.; Omary, M. A. *J. Phys. Chem. C* **2007**, *111*, 9522.

(34) Usón, R.; Laguna, A. *Organomet. Synth.* **1989**, *3*, 322.

Table 4. Details of Data Collection and Structure Refinement for Complexes 3–5

	3	4	5
chem formula	C ₅₂ H ₃₆ Au ₃ Br ₆ F ₂₄ NTl ₂	C ₅₂ H ₃₆ Au ₃ F ₂₄ I ₆ NTl ₂	C ₄₀ H ₃₆ Au ₂ Br ₄ F ₁₆ NTl
cryst habit	green plate	green prism	yellow prism
cryst size/mm	0.3 × 0.1 × 0.08	0.15 × 0.1 × 0.1	0.75 × 0.5 × 0.25
cryst syst	orthorhombic	triclinic	triclinic
space group	<i>Pbca</i>	<i>P</i> $\bar{1}$	<i>P</i> $\bar{1}$
<i>a</i> /Å	19.3225(1)	13.7380(2)	11.5160(2)
<i>b</i> /Å	25.5870(2)	15.2812(2)	13.9090(3)
<i>c</i> /Å	25.6821(2)	18.1752(3)	16.5790(4)
α /deg	90	102.704(1)	109.171(1)
β /deg	90	104.618(1)	96.968(1)
γ /deg	90	96.847(1)	104.685(1)
<i>V</i> /Å ³	12 697.35(15)	3539.44(9)	2364.76(9)
<i>Z</i>	82	2	2
<i>D</i> _c /g cm ⁻³	2.731	2.713	2.461
<i>M</i> _r	2609.92	2891.86	1752.64
<i>F</i> (000)	9440	2576	1612
<i>T</i> /°C	-100	-100	-100
2 θ _{max} /deg	54	54	56
μ (Mo K α)/mm ⁻¹	15.851	13.446	13.061
no. of rflns measd	182 931	56 203	33 734
no. of unique rflns	13 383	14 892	11 049
<i>R</i> _{int}	0.0671	0.0572	0.0901
<i>R</i> (<i>F</i> > 2 σ (<i>F</i>)) ^a	0.0427	0.0549	0.0658
<i>R</i> _w (<i>F</i> ² , all rflns) ^b	0.1128	0.1640	0.1819
no. of rflns used	13 383	14 892	11 049
no. of params	811	797	580
no. of restraints	73	86	58
<i>S</i> ^c	1.020	1.032	1.027
max residual electron density/e Å ⁻³	1.788	1.967	3.914

^a $R(F) = \sum ||F_o| - |F_c|| / \sum |F_o|$. ^b $R_w(F^2) = [\sum \{w(F_o^2 - F_c^2)^2\} / \sum \{w(F_o^2)^2\}]^{0.5}$; $w^{-1} = \sigma^2(F_o^2) + (aP)^2 + bP$, where $P = [F_o^2 + 2F_c^2]/3$ and a and b are constants adjusted by the program. ^c $S = [\sum \{w(F_o^2 - F_c^2)^2\} / (n - p)]^{0.5}$, where n is the number of data and p is the number of parameters.

under vacuum. Finally, the addition of *n*-hexane (20 mL) led to the precipitation of product **1** as a white solid. Yield: 90%. Anal. Calcd for **1** (C₂₈H₃₆AuBr₂F₈N): C, 37.56; H, 4.05; N, 1.56. Found: C, 36.48; H, 4.12; N, 1.50. ¹H NMR (75.5 MHz, CDCl₃, ppm): δ 3.05 (m, 2H, CH₂), 1.48 (m, 2H, CH₂), 1.31 (m, 2H, CH₂), 0.91 (t, 3H, CH₃). ¹⁹F NMR (282.4 MHz, CDCl₃, ppm): δ -114.6 (dd, 1F, F₁, ³J(F₁-F₂) = 33.9 Hz, ⁵J(F₁-F₄) = 13.4 Hz), -127.7 (dd, 1F, F₄, ³J(F₄-F₃) = 21.3 Hz), -158.3 (dd, 1F, F₂, ³J(F₂-F₃) = 19.7 Hz), -160.3 (dd, 1F, F₃). ES(+): *m/z* (%) 242 [NBu₄]⁺ (100). ES(-): *m/z* (%) 653 [Au(2-C₆BrF₄)₂]⁻ (100). FT-IR (Nujol): ν (2-C₆BrF₄) at 1612, 1594, 1078, and 817 cm⁻¹, ν (NBu₄⁺ C-N st) at 880 cm⁻¹.

Synthesis of NBu₄[Au(2-C₆F₄I)₂] (2). To a diethyl ether solution of Li(2-C₆F₄I) (30 mmol) at 203 K was added [AuCl(tht)] (3.20 g, 10 mmol). After 1 h of stirring, NBu₄Br (4 g, 12.5 mmol) was added and the reaction mixture was stirred at 203 K for 40 min. After 20 h of stirring at room temperature, a solid was separated by filtration and washed with water (3 × 5 mL), diethyl ether (3 × 5 mL), and *n*-hexane (3 × 5 mL). The solid was dissolved in dichloromethane and the solution concentrated under vacuum. Finally, the addition of *n*-hexane (20 mL) led to the precipitation of product **2** as an ocher solid. Yield: 93%. Anal. Calcd for **2** (C₂₈H₃₆AuI₂F₈N): C, 33.99; H, 3.67; N, 1.42. Found: C, 34.16; H, 3.56; N, 1.32. ¹H NMR (75.5 MHz, CDCl₃, ppm): δ 3.13 (m, 2H, CH₂), 1.56 (m, 2H, CH₂), 1.35 (m, 2H, CH₂), 0.94 (t, 3H, CH₃). ¹⁹F NMR (282.4 MHz, CDCl₃, ppm): δ -113.2 (dd, 1F, F₄, ³J(F₄-F₃) = 22.5 Hz, ⁵J(F₄-F₁) = 13.7 Hz), -115.0 (dd, 1F, F₁, ³J(F₁-F₂) = 33.8 Hz), -157.6 (dd, 1F, F₂, ³J(F₂-F₃) = 19.2 Hz), -160.4 (dd, 1F, F₃). ES(+): *m/z* (%) 242 [NBu₄]⁺ (100). ES(-): *m/z* (%) 747 [Au(2-C₆F₄I)₂]⁻ (100). FT-IR (Nujol): ν (2-C₆F₄I) at 1609, 1587, 1076, and 806 cm⁻¹, ν (NBu₄⁺ C-N st) at 880 cm⁻¹.

Synthesis of {NBu₄[Ti₂{Au(2-C₆BrF₄)₂}]_n (3). To a solution of NBu₄[Au(2-C₆BrF₄)₂] (**1**; 0.134 g, 0.15 mmol) in tetrahydrofuran (15 mL) was added TlPF₆ (0.052 g, 0.15 mmol). After 30 min of stirring, the solution was concentrated under vacuum to ca. 5 mL. Addition of toluene (15 mL) led to precipitation of TlPF₆ and NBu₄PF₆, which were separated by filtration. The filtrate was

evaporated to dryness, and complex **3** was obtained as a pale green solid, after washing with hexane (3 × 5 mL). Yield: 83%. Anal. Calcd for **3** (C₅₂H₃₆Au₃Br₆F₂₄NTl₂): C, 23.93; H, 1.39; N, 0.54. Found: C, 24.07; H, 1.44; N, 0.52. ¹H NMR (75.5 MHz, THF-*d*₈, ppm): δ 3.22 (m, 2H, CH₂), 1.65 (m, 2H, CH₂), 1.39 (m, 2H, CH₂), 0.98 (t, 3H, CH₃). ¹⁹F NMR (282.4 MHz, THF-*d*₈, ppm): δ -113.4 (dd, 1F, F₁, ³J(F₁-F₂) = 33.0 Hz, ⁵J(F₁-F₄) = 13.2 Hz), -127.8 (dd, 1F, F₄, ³J(F₄-F₃) = 20.6 Hz), -158.5 (dd, 1F, F₂, ³J(F₂-F₃) = 19.9 Hz), -160.6 (dd, 1F, F₃). ES(+): *m/z* (%) 242 [NBu₄]⁺ (100), 205 [Ti]⁺ (30). ES(-): *m/z* (%) 653 [Au(2-C₆BrF₄)₂]⁻ (100). FT-IR (Nujol): ν (2-C₆BrF₄) at 1617, 1595, 1088, and 823 cm⁻¹, ν (NBu₄⁺ C-N st) at 883 cm⁻¹.

Synthesis of {NBu₄[Ti₂{Au(2-C₆F₄I)₂}]_n (4). To a solution of NBu₄[Au(2-C₆F₄I)₂] (**2**; 0.148 g, 0.15 mmol) in tetrahydrofuran (15 mL) was added TlPF₆ (0.052 g, 0.15 mmol). After 2 h of stirring, the solution was concentrated under vacuum and toluene added to precipitate a white solid (TlPF₆ and the NBu₄PF₆), which was filtered off. Concentration of the solution and addition of dichloromethane (5 mL) led to precipitation of compound **4**, which was isolated as a yellow greenish solid after washing with dichloromethane (3 × 5 mL). Yield: 56%. Anal. Calcd for **4** (C₅₂H₃₆Au₃F₂₄I₆NTl₂): C, 21.60; H, 1.25; N, 0.48. Found: C, 21.77; H, 1.22; N, 0.54. ¹H NMR (75.5 MHz, THF-*d*₈, ppm): δ 3.22 (m, 2H, CH₂), 1.65 (m, 2H, CH₂), 1.39 (m, 2H, CH₂), 0.97 (t, 3H, CH₃). ¹⁹F NMR (282.4 MHz, THF-*d*₈, ppm): δ -113.4 (dd, 1F, F₄, ³J(F₄-F₃) = 22.0 Hz, ⁵J(F₄-F₁) = 13.8 Hz), -113.7 (dd, 1F, F₁, ³J(F₁-F₂) = 32.2 Hz), -157.7 (dd, 1F, F₂, ³J(F₂-F₃) = 18.9 Hz), -160.2 (dd, 1F, F₃). ES(+): *m/z* (%) 242 [NBu₄]⁺ (100), 205 [Ti]⁺ (40). ES(-): *m/z* (%) 747 [Au(2-C₆F₄I)₂]⁻ (100). FT-IR (Nujol): ν (2-C₆F₄I) at 1614, 1588, 1080, and 806 cm⁻¹, ν (NBu₄⁺ C-N st) at 886 cm⁻¹.

Synthesis of {NBu₄[Ti{Au(2-C₆BrF₄)₂}]_n (5). Method 1. To a solution of TlPF₆ (0.035 g, 0.1 mmol) in tetrahydrofuran (15 mL) was added NBu₄[Au(2-C₆BrF₄)₂] (**1**) (0.179 g, 0.2 mmol), and the solution turned pale yellow. After 45 min of stirring, the solution was concentrated under vacuum and a green oil appeared. Addition

of isopropyl alcohol (5 mL) led to the precipitation of compound **5**, which was isolated as a yellow solid after washing with isopropyl alcohol (3 × 5 mL). Yield: 85%.

Method 2. To a solution of {NBu₄[Ti₂{Au(2-C₆BrF₄)₂]₃]_n (**3**; 0.261 g, 0.1 mmol) in tetrahydrofuran (15 mL) was added NBu₄[Au(2-C₆BrF₄)₂] (**1**; 0.090 g, 0.1 mmol), and the solution turned pale yellow. After 45 min of stirring, the solvent was partially evaporated under vacuum and isopropyl alcohol was added to precipitate compound **5**, which was isolated as a yellow solid after washing with isopropyl alcohol (3 × 5 mL). Yield: 73%. Anal. Calcd for **5** (C₄₀H₃₆Au₂Br₄F₁₆NTl): C, 27.41; H, 2.07; N, 0.80. Found: C, 27.61; H, 2.17; N, 0.87. ¹H NMR (75.5 MHz, THF-*d*₈, ppm): δ 3.23 (m, 2H, CH₂), 1.65 (m, 2H, CH₂), 1.39 (m, 2H, CH₂), 0.98 (t, 3H, CH₃). ¹⁹F NMR (282.4 MHz, THF-*d*₈, ppm): δ -113.4 (dd, 1F, F₁, ³J(F₁-F₂) = 33.8 Hz, ⁵J(F₁-F₄) = 13.5 Hz), -128.2 (dd, 1F, F₄, ³J(F₄-F₃) = 20.9 Hz), -159.1 (dd, 1F, F₂, ³J(F₂-F₃) = 20.0 Hz), -161.7 (dd, 1F, F₃). ES(+): *m/z* (%) 242 [NBu₄]⁺ (100), 205 [Ti]⁺ (50). ES(-): *m/z* (%) 653 [Au(2-C₆BrF₄)₂]⁻ (100). FT-IR (Nujol): ν(2-C₆BrF₄) at 1613, 1595, 1083, and 822 cm⁻¹, ν(NBu₄⁺ C-N st) at 879 cm⁻¹.

Synthesis of {NBu₄[Ti{Au(2-C₆F₄I)₂]₂]_n (6**).** **Method 1.** To a solution of TIPF₆ (0.035 g, 0.1 mmol) in tetrahydrofuran (15 mL) was added NBu₄[Au(2-C₆F₄I)₂] (**2**; 0.198 g, 0.2 mmol). The solution turned yellow, and a solid started to precipitate. After 2 h of stirring the precipitation of compound **6** was complete and the complex was separated as a yellow solid by filtration and washed with tetrahydrofuran (3 × 5 mL). Yield: 95%.

Method 2. To a solution of {NBu₄[Ti₂{Au(2-C₆F₄I)₂]₃]_n (**4**; 0.289 g, 0.1 mmol) in tetrahydrofuran (15 mL) was added NBu₄[Au(2-C₆F₄I)₂] (**2**; 0.099 g, 0.1 mmol). The solution immediately turned yellow and a solid started to appear. After 2 h of stirring to complete the precipitation of **6**, the yellow solid was isolated by filtration and washed with tetrahydrofuran (3 × 5 mL). Yield: 88%. Anal. Calcd for **6** (C₄₀H₃₆Au₂F₁₆I₄NTl): C, 24.76; H,

1.87; N, 0.72. Found: C, 24.88; H, 1.91; N, 0.76. ES(+): *m/z* (%) 242 [NBu₄]⁺ (100), 205 [Ti]⁺ (20). ES(-): *m/z* (%) 747 [Au(2-C₆F₄I)₂]⁻ (100). FT-IR (Nujol): ν(2-C₆F₄I) at 1642, 1575, 1070, and 804 cm⁻¹, ν(NBu₄⁺ C-N st) at 887 cm⁻¹.

Crystallography. Crystals were mounted in inert oil on glass fibers and transferred to the cold gas stream of a Nonius Kappa CCD diffractometer equipped with an Oxford Instruments low-temperature attachment. Data were collected using monochromated Mo Kα radiation (λ = 0.710 73 Å), with scan types ω and φ and numerical absorption corrections (based on multiple scans). The structures were solved by direct methods and refined on *F*² using the program SHELXL-97.³⁵ All non-hydrogen atoms were refined anisotropically. In complex **3** the halogen atoms in ortho positions of one of the perhalophenyl rings are disordered with a 50% occupancy in each position (Br(2) and F(6) or F(2) and Br(6)). Hydrogen atoms were included using a riding model. Further details of the data collection and refinement are given in Table 4. Selected bond lengths and angles are collected in Tables 1–3, and crystal structures of complexes **3–5** are given in Figures 1–5.

Acknowledgment. This work was supported by the DGI(MEC)/FEDER (No. CTQ2007-67273-C02-02). M.M. and T.L. thank the CAR for a grant and a Colabora contract, respectively. We thank Prof. Mohammad Omary for helpful discussions.

Supporting Information Available: CIF files giving X-ray crystallographic data for the structural characterization of complexes **3–5**. This material is available free of charge via the Internet at <http://pubs.acs.org>.

OM8000586

(35) Sheldrick, G. M. SHELXL-97, A Program for Crystal Structure Refinement; University of Göttingen, Göttingen, Germany, 1997.